J. Appl Cryst. (1979). **12**, 312–315

The Thermal Expansion of 2*H*-MoS_2 and 2*H*-WSe_2 between 10 and 320 K

BY R. MURRAY AND B. L. EVANS

J. J. Thomson Physical Laboratory, University of Reading, Berkshire, England

(*Received* 20 *November* 1978; *accepted* 16 *January* 1979)

Abstract

The hexagonal cell dimensions a and c of 2*H*-MoS_2 and 2*H*-WSe_2 have been measured over the temperature range 10 to 320 K. In both compounds a increased linearly and c non-linearly with temperature, the linear coefficient of thermal expansion in the c direction being greater than that in the a direction for 2*H*-MoS_2. In 2*H*-WSe_2 the linear coefficients of thermal expansion in the a and c directions were approximately equal.

Introduction

MoS_2 and WSe_2 are crystalline semiconductors belonging to the large family of layer-like compounds whose crystal structure results from the stacking of sheets of hexagonally packed atoms in the sequence X–M–X, X–M–X. Within each X–M–X sandwich layer the metal (M) atom is bonded to six nearest-neighbour (X) atoms in trigonal prismatic or octahedral coordination depending upon the ionic ratio, r_{M^+}/r_{X^-}, and the fractional ionic character, f_i (Gamble, 1974), where $f_i = 1-\exp\left[-\frac{1}{4}(X_M - X_X)^2\right]$ and X_M, X_X are the electronegativities of the metal (M) and chalcogen (X) atoms, respectively.

In MoS_2 and WSe_2 the metal atom has trigonal prismatic coordination within the sandwich layer and a number of structural polytypes are possible depending upon the way in which the layers are stacked one upon the other (Zvyagin & Soboleva, 1967). The most common polytypes are the hexagonal 2*H*-MoS_2, where the stacking sequence is $ABA|BAB$ in the $(11\bar{2}0)$ section, and rhombohedral 3*R*-MoS_2 where the stacking sequence is $ABA|BCB|CAC$ in the $(11\bar{2}0)$ section; the vertical strokes denote layer–layer separation.

The bonding between sandwich layers is comparatively weak with the result that MoS_2 and WSe_2 crystals show easy cleavage in (00.1). The surfaces of MoS_2 crystals grown directly from the powder compound show well-defined hexagonal growth spirals (Al-Hilli & Evans, 1972*a*) and X-ray powder lines which can be identified in terms of the $P6_3/mmc$ (D^4_{6h} space group) 2*H* crystal structure. Crystals of MoS_2 grown by halogen vapour transport show triangular surface-growth features and the X-ray powder lines correspond to the (3*R*) rhombohedral structure in which, referred to the hexagonal lattice, the a parameter of the unit cell is similar to that of the 2*H* polytype but the c parameter is about 1·5 times as great (Al-Hilli & Evans, 1972*a*).

WSe_2 crystals grown directly from the powder occur as the 2*H* polytype and show well-defined hexagonal growth features (Al-Hilli & Evans, 1972*a*). Crystals grown by bromine vapour transport have the form of thin buckled plates with no obvious growth features; the X-ray patterns however are those of the 2*H* polytype.

The room temperature d.c. conductivity $\sigma_\perp$ (*i.e.* $\perp$c, parallel to the crystal layers) in 2*H*-MoS_2 and 2*H*-WSe_2 is typically 100 $\sigma_\parallel$, where $\sigma_\parallel$ is the conductivity in the c direction. At temperatures above *ca* 800 K the conductivity $\sigma_\perp$ increases rapidly with rise in temperature T(K) and the slope $m(=E_a/2k)$ of the linear ln $\sigma_\perp$ *versus* $1/T$ graphs gives the thermal activation energy E_a. In crystals grown directly from the powder $E_a = 1{\cdot}27 \pm 0{\cdot}06$ eV in n-type MoS_2 (El-Mahalawy & Evans, 1977) and $1{\cdot}32 \pm 0{\cdot}08$ eV in p-type WSe_2 (Davey & Evans, 1972). These values of E_a are probably the thermal counterparts of the $E_\perp$ c direct optical energy gaps (77 K) which occur at 1·791 eV in MoS_2 (Neville & Evans, 1976) and 1·782 eV in WSe_2 (Bradley, Katayama & Evans, 1972). Energy gaps of this magnitude occur in the calculated band structures (Bromley, Murray & Yoffe, 1972; Harper & Edmondson, 1971; Huisman, de Jonge, Haas & Jellinek, 1971; Mattheiss, 1973; Kasowski, 1973) but the transitions giving rise to the optical absorption have not been positively identified. The optical absorption edge in the 3*R*-MoS_2 polytype occurs at a lower energy than in the 2*H* polytype (Clark & Williams, 1968). Similarly the excitonic spectra which comprise the absorption edge in 2*H*-MoS_2 and 2*H*-WSe_2 have the properties of three- rather than two-dimensional excitons. Thus the anisotropy in these compounds, although severe, is not sufficiently extreme for the crystal to be represented by a single sandwich layer.

The variation in cell dimensions of MoS_2 and WSe_2 with temperature has been measured in order to determine (*a*) whether the 2*H* structure present at room temperature persists to the low-temperature region and (*b*) the relative importance of electron–phonon interaction and thermal expansion in the observed temperature shift of the fundamental optical absorption edge. The numerical values of the thermal expansion complement the published values of thermal expansion in the high temperature (293–1073 K) region (El-Mahalawy & Evans, 1976).

Preparation of MoS_2 and WSe_2 crystals

MoS_2 and WSe_2 compounds were prepared from elements having the following purities (wt%) Mo (99·99),

0021-8898/79/030312-04$01.00

W(99·95), S(99·999) Se(99·99). Stoichiometric amounts of the powdered elements were introduced into a silica ampoule which was evacuated to a pressure of 1·333 $\times 10^{-4}$ Pa before sealing. The ampoule was vibrated for 30 min to ensure complete mixing of the contents. The mixture was then distributed evenly along the length of the horizontally-held ampoule, which was slowly heated over a period of 5 h, to a temperature of 973 K and maintained at this temperature for 24 h. At this stage the reaction product was in the form of a free-flowing fine black powder. The constituents of the sealed ampoule were again vibrated for 30 min before the ampoule was returned to the furnace and maintained in an appropriate temperature gradient (Al-Hilli & Evans, 1972*a*) around 1273 K for two weeks. At the end of this time single crystals were found growing from the polycrystalline cake. Quantitative analysis has shown that crystals grown in this way have the correct composition, the only detectable impurity being 0·03 wt% Si.

The single crystals of MoS_2 and WSe_2 were then ground, using a pestle and mortar, into a particle size suitable for filling a 0·3 mm-diameter silica X-ray capillary tube.

Experimental method

X-ray powder diffraction patterns (Cu $K\alpha$ radiation) were obtained with a 190 mm powder camera incorporating a continuous-flow helium cryostat. The temperature of the specimen in the cryostat could be maintained at any temperature in the range 4·2 to 290 K by adjusting the current through an electric heater wound around the sample block of the cryostat. The sample temperature was approximately given by a cryogenic linear temperature sensor (CLTS) attached, by low-temperature adhesive, to the sample block. The powder sample was mixed with 98% purity copper powder before filling the capillary tube so that the powder pattern consisted of copper and MoS_2 (or WSe_2) diffraction lines. The real sample temperature was determined from the measured copper unit-cell dimensions and the published values of the copper lattice parameter (White, 1973) at low temperatures. Halving the X-ray tube current (normally 11 mA at 22kV) showed that there was no preferential beam heating of the copper or the compound.

The MoS_2 and WSe_2 powder-pattern lines at room temperature were indexed with reference to the previously published values of the hexagonal cell dimensions a and c. Accurate values of a and c at room and all other temperatures were then obtained by a computer procedure which minimised the difference between calculated and measured $\sin^2\theta$ for all lines of the powder pattern. Experimental values of a and c at different temperatures are shown in Figs. 1 and 2 for $2H$-MoS_2 and $2H$-WSe_2. The curves through the experimental points represent the polynomial

$$x_t = x_0 + x_1 t + x_2 t^2 + x_3 t^3 + \ldots, \qquad (1)$$

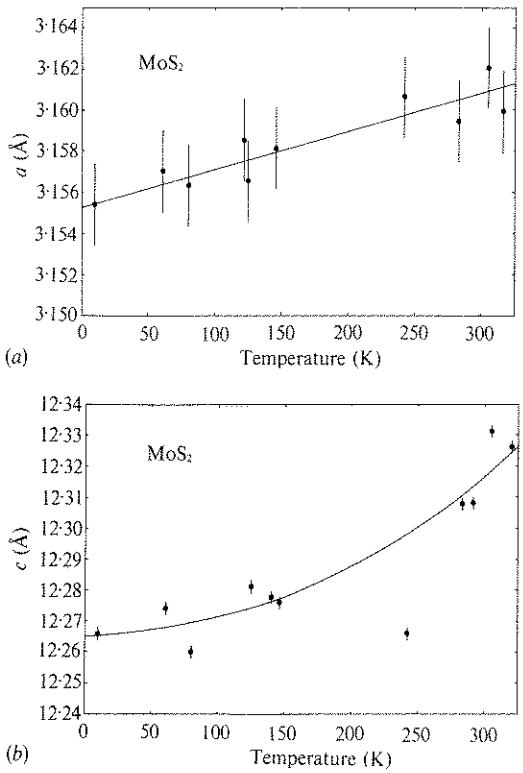

Fig. 1. The cell parameters (*a*) in the *a* direction and (*b*) in the *c* direction of $2H$-MoS_2 over the temperature range 0 to 320 K.

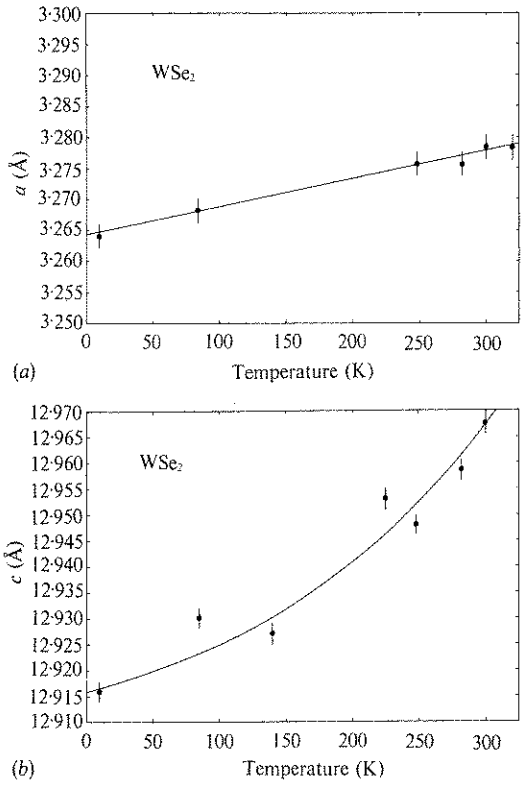

Fig. 2. The cell parameters (*a*) in the *a* direction and (*b*) in the *c* direction of $2H$-WSe_2 over the temperature range 0 to 320 K.

giving the best least-squares fit to the experimental values. Here t is the temperature in K and the ratio x_1/x_0 gives the principal linear coefficient of thermal expansion in the a or c direction.

Cell dimensions of MoS_2

All the powder lines of MoS_2 at room temperature (300 K) could be identified in terms of a hexagonal unit cell having dimensions $a=3{\cdot}159\pm0{\cdot}002$, $c=12{\cdot}307\pm0{\cdot}002$ Å, compared with the previously reported values; $a=3{\cdot}160$, $c=12{\cdot}295$ Å (Jellinek, 1962), $a=3{\cdot}140\pm0{\cdot}008$, $c=12{\cdot}327\pm0{\cdot}008$ Å (Al-Hilli & Evans, 1972*b*), $a=3{\cdot}1622\pm0{\cdot}007$, $c=12{\cdot}301\pm0{\cdot}002$ Å (El-Mahalawy & Evans, 1976). The measured values of a and c for 2H-MoS_2 at different temperatures t K are shown in Fig. 1. The curves through the experimental points giving the temperature dependence of a and c are

$$a=3{\cdot}1553+1{\cdot}553\times10^{-5}\,t, \qquad (2)$$

$$c=12{\cdot}265+2{\cdot}28\times10^{-4}t+1{\cdot}15\times10^{-6}t^2, \qquad (3)$$

which gives the principal linear coefficients of thermal expansion as $\alpha_a=4{\cdot}922\times10^{-6}$ and $\alpha_c=18{\cdot}58\times10^{-6}$/K over the temperature range 10 to 300 K compared with $\alpha_a=1{\cdot}9\times10^{-6}$, $\alpha_c=8{\cdot}65\times10^{-6}$/K over the temperature range 300 to 1100 K (El-Mahalawy & Evans, 1976).

Cell dimensions of WSe_2

All the powder lines of WSe_2 at room temperature could be identified in terms of a hexagonal unit cell having dimensions $a=3{\cdot}278\pm0{\cdot}002$, $c=12{\cdot}962\pm0{\cdot}002$ Å. Previously reported values for WSe_2; $a=3{\cdot}282\pm0{\cdot}004$, $c=12{\cdot}937\pm0{\cdot}01$ Å (Al-Hilli & Evans, 1972*b*), $a=3{\cdot}29$, $c=12{\cdot}97$ Å (Glemser, Sauer & König, 1948), $a=3{\cdot}2781\pm0{\cdot}0007$, $c=12{\cdot}9505\pm0{\cdot}002$ Å (El-Mahalawy & Evans, 1976). The measured values of a and c for WSe_2 at different temperatures in the range 10 to 350 K are given in Fig. 2. The curves drawn through the experimental points are

$$a=3{\cdot}264+4{\cdot}717\times10^{-5}t, \qquad (4)$$

$$c=12{\cdot}916+1{\cdot}77\times10^{-4}t-3{\cdot}9\times10^{-7}t^2, \qquad (5)$$

where t is the temperature in K and the principal linear coefficients of thermal expansion are $\alpha_a=1{\cdot}445\times10^{-5}$ and $\alpha_c=1{\cdot}374\times10^{-5}$/K over the temperature range 10 to 300 K. Previously published values give $\alpha_a=0{\cdot}68\times10^{-5}$, $\alpha_c=1{\cdot}06\times10^{-5}$/K (Brixner, 1963) and $\alpha_a=1{\cdot}108\times10^{-5}$, $\alpha_c=1{\cdot}672\times10^{-5}$/K (El-Mahalawy & Evans, 1976) over the temperature range 300 to 1000 K.

Discussion

For MoS_2 the principal linear coefficient of thermal expansion $\alpha_c>\alpha_a$ which is consistent with the relative inter- and intra-layer bond strengths (Evans, 1976). Similarly the compressibility β of 2H-MoS_2 is greater in the c direction than in the a direction (Flack, 1972). The thermal expansion ratio α_c/α_a of WSe_2 ($\simeq1$) is much smaller than that of MoS_2 (3·6) which presumably reflects the differences in the interatomic bonding forces between the two compounds.

From a knowledge of the thermal expansion coefficients of 2H-MoS_2 it is possible to determine the relative contributions of the thermal expansion and electron–phonon interaction to the temperature dependence of an electron interband transition energy. Since the energy of a transition is a function of the pressure, temperature and volume of the solid, the temperature dependence of the transition is given by Grant, Wilson & Yoffe (1972);

$$\left(\frac{\partial E}{\partial T}\right)_p=\left(\frac{\partial E}{\partial T}\right)_V-\left(\frac{\alpha_c+2\alpha_a}{\beta_c+2\beta_a}\right)\left(\frac{\partial E}{\partial p}\right)_T, \qquad (6)$$

where the thermal expansion coefficients $\alpha=\frac{1}{V}\left(\frac{\partial V}{\partial T}\right)_p$ in the a and c directions are given above and in the case of 2H-MoS_2 the isothermal compressibility $\beta=-\frac{1}{V}\left(\frac{\partial V}{\partial p}\right)_T$ in the a and c directions has been measured (Flack, 1972).

In 2H-MoS_2 the optical absorption edge for light propagated parallel to the crystal c (optic) axis consists of two series (A & B) of absorption lines due to direct transitions into delocalised exciton states (Frindt & Yoffe, 1963; Evans & Young, 1965). Fig. 3 shows the measured temperature dependence of exciton absorption peaks A_1, A_2 and B_1 in a 2H-MoS_2 crystal 127 nm thick over the temperature range 15 to 300 K. It can be seen that there is little difference in the temperature dependence of the A and B series excitons for which $(\partial E/\partial T)_p=-0{\cdot}3$ meV/K, between 80 and 300 K. Hydrostatic pressure measurements on 2H-MoS_2 (300 K) have found $(\partial E/\partial p)_T=2{\cdot}0\times10^{-8}$ meV/Pa for the optical absorption edge for pressures up to 6×10^8 Pa (Grant, Wilson & Yoffe, 1972). Substituting these values for $(\partial E/\partial T)_p$ and $(\partial E/\partial p)_T$ in equation (6), together with the room temperature values of the compressibility $\beta_a=3{\cdot}3\times10^{-12}$/Pa and $\beta_c=17\times10^{-12}$/Pa (Flack 1972), it is found that the last term in equation (6) is 0·022 meV/K at room temperature. The temperature shift of A_1, *viz* −0·3 meV/K is thus primarily due to the electron lattice term $(\partial E/\partial T)_V$ with the lattice expansion having comparatively little effect. Below 80 K the temperature shift of A_1 reduces becoming immeasurably small below 15 K. Grant, Wilson & Yoffe (1972) have measured $(\partial E/\partial p)_T$ at 80 K to be $1{\cdot}4\times10^{-8}$ meV/Pa but without values for the compressibilities β_a, β_c in this low-temperature range it is impossible to determine the relative importance of the lattice expansion and electron–lattice interaction terms in equation (6).

Below room temperature the activation energy for electrical conduction in 2H-MoS_2 indicates an energy gap of 0·47 eV in the electron energy band structure. (El-Mahalawy & Evans, 1977). This energy gap is much smaller than the direct gaps associated with the exciton

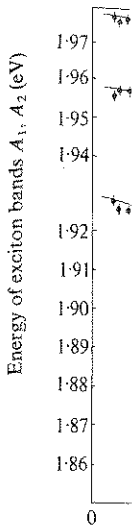

Fig. 3. The en
function of
thick.

spectra and
indirect g
(Goldberg,
gap associ
(Harper, 19
Pa) of the
$\times10^{-8}$ meV
of opposite
supports th
tron energy
The temp
in 2H-WSe
range 77 t
(Bradley, K
Yoffe (1972
the A_1 peak
vapour tran
$\times10^{-14}$ eV
lities β_a, β_c
could be gu
mately equ
were of the
for 2H-MoS
2H-WSe_2,

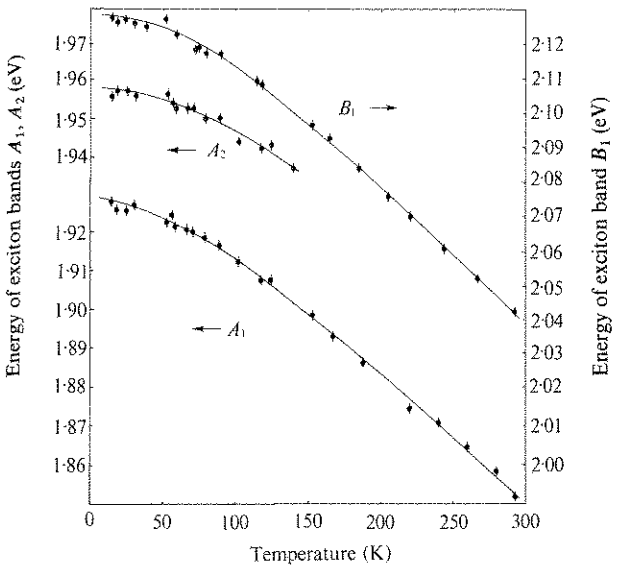

Fig. 3. The energies of exciton absorption bands A_1, A_2 and B_1 as a function of temperature in a single crystal of 2*H*-MoS_2, 127 nm thick.

spectra and has been tentatively attributed either to an indirect gap forming the absorption threshold (Goldberg, Beal, Levy & Davis, 1975) or to an energy gap associated with unequal layer–layer stacking (Harper, 1974). The pressure dependence (4 to 30×10^8 Pa) of the electrical conduction is $(\partial E/\partial p)_T = -3{\cdot}8 \times 10^{-8}$ meV/Pa (El-Mahalawy & Evans, 1978) which is of opposite sign to that of the direct optical gap and this supports the conclusion that it involves different electron energy bands.

The temperature dependence of the A_1 exciton peak in 2*H*-WSe_2 has been measured over the temperature range 77 to 300 K giving $(\partial E/\partial T)_p = -0{\cdot}5$ meV/K (Bradley, Katayama & Evans, 1972). Grant, Wilson & Yoffe (1972) have measured the pressure dependence of the A_1 peak of 2*H*-WSe_2 crystals grown with iodine as vapour transport and obtained the result $(\partial E/\partial p)_T = 1{\cdot}1 \times 10^{-14}$ eV/Pa. No measurements of the compressibilities β_a, β_c have been made on 2*H*-WSe_2 although it could be guessed that since $\alpha_c \simeq \alpha_a$, these are approximately equal. Assuming that the values of β_a and β_c were of the same order of magnitude for 2*H*-WSe_2 as for 2*H*-MoS_2 then the same conclusion would hold for 2*H*-WSe_2, namely that at room temperature the electron–lattice interaction is predominantly responsible for the shift of the A_1 exciton peak with temperature.

References

Al-Hilli, A. A. & Evans, B. L. (1972*a*). *J. Cryst. Growth*, **5**, 93–101.

Al-Hilli, A. A. & Evans, B. L. (1972*b*). *J. Appl. Cryst.* **5**, 221–224.

Bradley, D. J., Katayama, Y. & Evans, B. L. (1972). *Solid State Commun.* **11**, 1695–1698.

Brixner, L. H. (1963). *J. Electrochem. Soc.* **110**, 289–292.

Bromley, R. A., Murray, R. B. & Yoffe, A. D. (1972). *J. Phys. C*, **5**, 759–778.

Clark, A. & Williams, R. H. (1968). *J. Phys. D*, **1**, 1222–1223.

Davey, B. & Evans, B. L. (1972). *Phys. Status Solidi A*, **13**, 483–491.

El-Mahalawy, S. H. & Evans, B. L. (1976). *J. Appl. Cryst.* **9**, 403–406.

El-Mahalawy, S. H. & Evans. B. L. (1977). *Phys. Status Solidi B*, **79**, 713.

El-Mahalawy, S. H. & Evans, B. L. (1978). *Phys. Status Solidi B*, **86**, 151.

Evans, B. L. (1976). *Optical and Electrical Properties*, Chapter 1. Dordrecht; Reidel Publishing Co.

Evans, B. L. & Young, P. A. (1965). *Proc. R. Soc. London Ser. A*, **284**, 402.

Flack, H. D. (1972). *J. Appl. Cryst.* **5**, 137–138.

Frindt, R. F. & Yoffe, A. D. (1963). *Proc. R. Soc. London Ser. A*, **273**, 69.

Gamble, F. R. (1974). *J. Solid State Chem.* **9**, 358–361.

Glemser, O., Sauer, H. & König, P. (1948). *Z. Anorg. Allg. Chem.* **257**, 241–244.

Goldberg, A. M., Beal, A. R., Levy, F. A. & Davis, E. A. (1975). *Philos. Mag.* **32**, 367.

Grant, A. J., Wilson, J. A. & Yoffe, A. D. (1972). *Philos. Mag.* **25**, 625–636.

Harper, P. G. (1974). *J. Phys. C*, **7**, 1247–1256.

Harper, P. G. & Edmondson, D. R. (1971). *Phys. Status Solidi*, **44**, 59–69.

Huisman, R., de Jonge, R., Haas, C. & Jellinek, F. (1971). *J. Solid State Chem.* **3**, 56–59.

Jellinek, F. (1962). *Ark. Kemi*, **20**, 447–449.

Kasowski, R. V. (1973). *Phys. Rev. Lett.* **30**, 1175–1178.

Mattheiss, L. F. (1973). *Phys. Rev. Lett.* **30**, 784–787.

Neville, R. A. & Evans, B. L. (1976). *Phys. Status Solidi B*, **73**, 597–606.

White, G. K. (1973). *J. Phys. D*, **6**(II), 2070–2080.

Zvyagin, B. B. & Soboleva, S. V. (1967). *Sov. Phys. Crystallogr.* **12**, 46–52.